THE ASTROPHYSICAL JOURNAL, 214:488–497, 1977 June 1

SELF-SIMILAR COLLAPSE OF ISOTHERMAL SPHERES AND STAR FORMATION

FRANK H. SHU
Astronomy Department, University of California, Berkeley
Received 1976 June 10; revised 1976 September 27

ABSTRACT

We consider the problem of the gravitational collapse of isothermal spheres by applying the similarity method to the gas-dynamic flow. We argue that a previous solution obtained by Larson and Penston to describe the stages *prior* to core formation is physically artificial; however, we find that the flow *following* core formation does exhibit self-similar properties.

The latter similarity solution shows that the inflow in the dense central regions proceeds virtually at free-fall before the material is arrested by a strong radiating shock upon impact with the surface of the core. Two types of similarity solutions are obtained: one is the prototype for starting states which correspond to unstable hydrostatic equilibrium; the other, for states where the mass of the cloud slightly exceeds the maximum limit allowable for hydrostatic equilibrium. In both cases, an r^{-2} law holds for the density distribution in the static or nearly static outer envelope, and an $r^{-3/2}$ law holds for the freely falling inner envelope. Rapid infall is initiated at the head of the expansion wave associated with the dropping of the central regions from beneath the envelope. A numerical example is presented which is shown to be in good agreement with the envelope dynamics obtained in previous studies of star formation using hydrodynamic codes.

Subject headings: hydrodynamics — stars: formation

I. INTRODUCTION

The gravitational collapse of a gas cloud has received considerable theoretical attention in the astrophysical literature, particularly in connection with the problem of star formation (see the reviews by Hayashi 1966; Spitzer 1968; Larson 1973; and Mestel 1974). Although magnetic fields and rotation probably play important roles, some aspects of the problem are most simply studied by ignoring these factors in the idealized context of spherical collapse. For the latter problem, the critical assumption is that radiative losses offset compressional heating and keep the contracting gas cloud relatively cold and nearly isothermal (Gaustad 1963).

In the earlier discussions it had been argued that three-dimensional contraction under isothermal conditions leads to an ever increasing imbalance of gravitational forces over pressure forces, and, thus, that such contraction would lead eventually to a free-fall state and to gravitational fragmentation (see, e.g., Hunter 1967). Recent numerical work shows that pressure gradients do play an important role in the early phases of the collapse process (McNally 1964; Bodenheimer and Sweigart 1968; Penston 1969*b*; Larson 1969; Appenzeller 1972; Westbrook and Tarter 1975). They help to establish conditions whereby a central core collapses well before a more extended envelope.

The hydrodynamic-code calculations show that prior to core formation, an r^{-2} law develops for the envelope density distribution. Larson (1969) and Penston (1969*a*) attempted to explain this phenomenon in terms of a similarity solution for the early stages of the gas-dynamic flow. Despite the good intentions of their approach, this attempt failed to produce acceptable solutions for the collapse problem. The difficulty arises because the beginning phase of an arbitrary initial-value problem is usually not amenable to a similarity analysis. For example, in the theory of the evolution of supernova remnants, the *approach* to the Taylor-Sedov blast wave solution from a non-point explosion ("Phase I" in the terminology of Woltjer 1972) generally depends on the specific details of the initial explosive process. The usefulness of the Taylor-Sedov solution depends on the convergence, asymptotically in time (until radiative losses become important), of a wide class of explosive flows to the ideal similarity solution *independent* of the details of the initial conditions, as long as they satisfy certain general requirements.

In the present context, difficulties arise because only very special initial and boundary conditions could lead to the Larson-Penston flow. To see this, we recall that the Larson-Penston similarity solution has the following characteristics: (*a*) the flow at large radii is directed inward at 3.3 times the speed of sound (leading to an r^{-2} distribution for the density in the envelope); (*b*) the density field at large radii is 4.4 times the value appropriate to hydrostatic equilibrium; (*c*) the velocity profile goes monotonically and smoothly (i.e., without a shock) to zero at the origin. Clearly, properties (*a*) and (*b*) are numerically ad hoc. Moreover, although property (*c*) may qualitatively describe the gradual acceleration of the *innermost* regions of numerically computed flows during the early stages before core formation, flow with the property (*a*) of being fed in supersonically at an outer boundary can generally be brought to rest smoothly (but probably not stably)

only by an artificial arrangement of self-gravity and pressure gradient.

How, then, can we understand the observed establishment of an r^{-2} law under a wide variety of initial conditions? The physical reason is simple even if the mathematics is not: the convergence to an r^{-2} law represents the tendency of an isothermal self-gravitating gas to approach, as closely as possible, detailed mechanical balance. This tendency will be satisfied as long as different parts of the cloud can communicate acoustically with one another, i.e., as long as the initial conditions allow the early phases of the flow to occur subsonically (see Bodenheimer and Sweigart 1968). Once an r^{-2} law has been (nearly) established without the generation of considerable fluid velocities, the subsequent collapse flow occurs in a self-similar manner. Prior to the latter phase, the flow will generally not be self-similar. Before we begin a formal discussion of the similarity solution, we make some clarifying remarks concerning the importance of an early subsonic phase for establishing the assumed "initial conditions" of our similarity solution.

Pressure-free spheres released from rest with a uniform density remain uniform throughout the collapse (except when perturbed; see Lin, Mestel, and Shu 1965 and Hunter 1967). The development of a nonuniform density profile in the presence of finite gas pressure, even if the initial state is uniform, then seemingly presents a puzzle since gas pressure (in contrast with self-gravity) tends to smooth inhomogeneities, not to enhance them. The resolution of the paradox is that the numerical starting conditions adopted are usually not very far removed from marginal gravitational stability, and this state allows an early phase of subsonic readjustment to the imposed boundary conditions; whereas in pressure-free collapse the acoustic speed is assumed from the outset to be negligible compared to the fluid velocities generated by self-gravity.

To elaborate, consider, first, the important case of an extreme early subsonic phase—namely, starting states which are in perfect hydrostatic equilibrium. For an isothermal cloud embedded in an external medium of pressure $P_{\rm ext}$, hydrostatic equilibrium is possible providing the mass of the cloud does not exceed the critical value (Ebert 1955, Bonnor 1956):

$$M_{\rm crit} = 1.18 \frac{a^4}{G^{3/2}} P_{\rm ext}^{-1/2}, \qquad (1)$$

where $a = (kT/m)^{1/2}$ is the isothermal speed of sound inside the cloud. For clouds with masses less than $M_{\rm crit}$, both stable and unstable equilibria are possible. The stable clouds are characterized by a degree of central concentration which is less than the critical Bonnor-Ebert sphere; the unstable states, by a degree of central concentration which is greater (Spitzer 1968). In the limit of infinite central concentration, the unstable equilibria approach the "singular isothermal sphere" which has the density and mass distributions:

$$\rho(r) = \frac{a^2}{2\pi G} r^{-2}, \quad M(r) = \frac{2a^2}{G} r. \qquad (2)$$

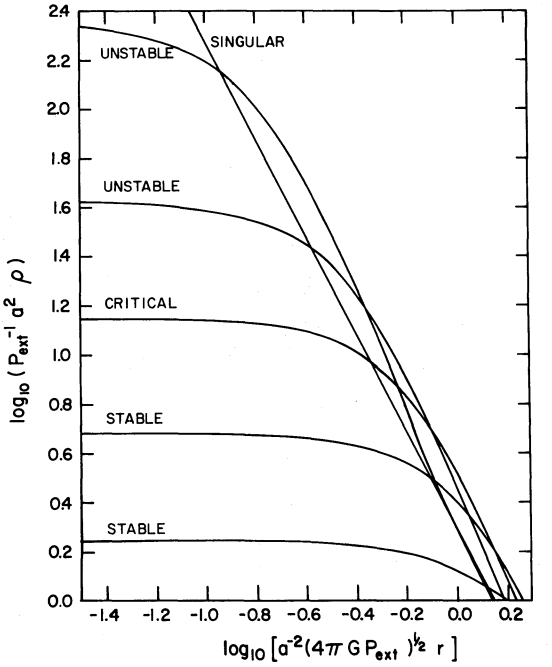

FIG. 1.—Density distributions of bounded isothermal spheres. The outer radius of each sphere is given by the intercept of the corresponding curve with the abscissa. The curve marked "critical" denotes the sphere with the maximum mass consistent with hydrostatic equilibrium at a given external pressure. Hydrostatic spheres which are less centrally concentrated than the critical Bonnor-Ebert state are gravitationally stable; those which are more centrally concentrated are gravitationally unstable. In the limit of infinite central concentration, the latter spheres approach the singular solution.

(See Chandrasekhar 1957, pp. 155–170.) The singular solution (2), truncated at a boundary pressure $P_{\rm ext}$, has a total radius R and a total mass $M(R)$ given by

$$R = \frac{a^2}{(2\pi G)^{1/2}} P_{\rm ext}^{-1/2},$$

$$M(R) = \left(\frac{2}{\pi}\right)^{1/2} \frac{a^4}{G^{3/2}} P_{\rm ext}^{-1/2}, \qquad (3)$$

which are, respectively, factors of 0.82 and 0.68 smaller than the critical Bonnor-Ebert sphere. The density profiles of several of these equilibrium states are plotted in Figure 1. Notice that the density distributions in the outer envelopes of the critical and unstable states all resemble the r^{-2} distribution that characterizes the singular isothermal sphere. Notice also that the unstable isothermal spheres all have ratios of central to surface density which exceeds 14.3, the value for the critical Bonnor-Ebert sphere (see also Table 4 of Shu *et al.* 1972). Thus, starting conditions which involve unstable equilibria that will collapse, given a small perturbation, necessarily all have substantial central concentration to begin with; this central concentration will only be enhanced in the collapse.

Consider, next, starting conditions where the mass of the cloud exceeds the critical Bonnor-Ebert mass (1)

only slightly. No hydrostatic state of equilibrium is now accessible to the system—stable or unstable—and the cloud *must* evolve dynamically. The sound travel time in the outer envelope will generally be short in comparison with the gravitational time scale; hence, the small discrepancy between gravity and pressure gradients will be spread by a slow subsonic flow as smoothly as possible. As we shall see in § IIc, this dynamical process still gives an r^{-2} law for the density distribution in the outer envelope. (See also the discussion of Bodenheimer and Sweigart 1968 for an illuminating discussion of the r^{-2} law obtained in the flow calculations using hydrodynamical codes.) In contrast, the gravitational collapse of the central regions occurs much more quickly, leading to a very strong central concentration for the collapsing configuration. As time proceeds and transients decay, we expect the collapse properties to resemble those appropriate to singular isothermal spheres. As we shall see, the collapse of singular spheres proceeds in a self-similar manner. We now begin our mathematical analysis; the physically motivated reader may prefer to skip to § III for a specific numerical example.

II. SIMILARITY SOLUTIONS FOR SELF-GRAVITATING ISOTHERMAL FLOW

We begin by writing the fluid equations in Eulerian form. For spherically symmetric flow, mass conservation can be expressed in terms of mass shells,

$$\frac{\partial M}{\partial t} + u\frac{\partial M}{\partial r} = 0\,, \quad \frac{\partial M}{\partial r} = 4\pi r^2 \rho\,, \tag{4}$$

where $M(r, t)$ is the total mass (core plus envelope) inside radius r at time t. The relations (4) are equivalent to the usual equation of continuity,

$$\frac{\partial \rho}{\partial t} + \frac{1}{r^2}\frac{\partial}{\partial r}(r^2 \rho u) = 0\,. \tag{5}$$

For ideal isothermal flow, the force equation reads

$$\frac{\partial u}{\partial t} + u\frac{\partial u}{\partial r} = -\frac{a^2}{\rho}\frac{\partial \rho}{\partial r} - \frac{GM}{r^2}\,. \tag{6}$$

The equations (4)–(6) are formally invariant to the time-reversal transformation: $t \to -t$, $\rho \to \rho$, $u \to -u$. The formal time-reversal invariance would, of course, be broken by the introduction of shocks which are generally needed to complete a realistic solution of an accretion problem.

For simplicity, let us first concentrate on the part of the flow which is well removed from the outer boundary so that the internal pressures are much larger than $P_{\rm ext}$. We further assume that the collapse occurs over many orders of magnitude in density so that the central object (accreting protostar) has negligible dimensions in comparison with the region of accretion flow. Then, the only dimensional quantities of the problem are the gravitational constant G, the isothermal sound speed a, the local radius r, and the instantaneous time t.[1] From these quantities, simple dimensional analysis gives the similarity variable as

$$x = r/at\,. \tag{7}$$

We now look for similarity solutions of the form

$$\rho(r, t) = \frac{\alpha(x)}{4\pi G t^2}\,, \quad M(r, t) = \frac{a^3 t}{G} m(x)\,,$$

$$u(r, t) = av(x)\,, \tag{8}$$

where $t = 0$ defines the instant when the mass of the core, $M(0, t)$, is zero. The density distribution will be well behaved as $t \to 0$ provided $\alpha(x)$ goes to zero at least as fast as x^{-2} at large $|x|$. The instant $t = 0$ corresponds to the instant of core formation for the collapse problem. For the wind problem, the instant $t = 0$ corresponds to the final instant when the central mass has blown completely away. Hence, for inflow problems, t, x, and m are positive while v is negative; for outflow problems, t, x, and m are negative while v is positive. To prevent confusion, we always talk in terms of inflow and refer to $t = 0$ as the "initial instant." The formal solutions which we obtain in this manner that correspond to time-reversed winds can be converted to their proper outflow context by reversing the signs of t, x, v, and m.

The substitution of equations (8) into equations (4) now yields the ordinary differential equations

$$m - x\frac{dm}{dx} + v\frac{dm}{dx} = 0\,, \quad \frac{dm}{dx} = x^2\alpha\,. \tag{9}$$

The term dm/dx can be eliminated from the above relations to give

$$m = x^2\alpha(x - v)\,. \tag{10}$$

This formula plus some straightforward manipulation now allows us to express equations (5) and (6) as the coupled set of ordinary differential equations,

$$[(x - v)^2 - 1]\frac{dv}{dx} = \left[\alpha(x - v) - \frac{2}{x}\right](x - v)\,, \tag{11}$$

$$[(x - v)^2 - 1]\frac{1}{\alpha}\frac{d\alpha}{dx} = \left[\alpha - \frac{2}{x}(x - v)\right](x - v)\,. \tag{12}$$

Apart from some notational differences and sign conventions, equations (11) and (12) are equivalent to the equations derived previously by Larson (1969) and Penston (1969*a*).

a) Singular Solutions

An exact analytic solution of equations (10)–(12) is given by the static state

$$v = 0\,, \quad \alpha = 2/x^2\,, \quad m = 2x\,. \tag{13}$$

[1] This statement is strictly true only for the collapse of extended isothermal spheres (occupying infinite volume and possessing infinite mass). The collapse of a bounded isothermal sphere must eventually depend on the total mass of the system, or equivalently, on $P_{\rm ext}$ (see § III).

In dimensional units, the above set corresponds to the time-independent singular solution (2). This singular solution is the only hydrostatic solution of the isothermal sphere problem which is self-similar; consequently, if it is used as the "initial state," we can obtain a similarity solution which is an exact solution of the collapse problem for all times before the presence of the outer boundary begins to play a dynamic role (see § II*c*).

Another apparent singular solution of equations (11) and (12) is given by

$$x - v = 1\,, \quad \alpha = 2/x\,. \tag{14}$$

(The conjugate set: $x - v = -1$, $\alpha = -2/x$ corresponds to negative x.) However, the second solution (14) is mathematically extraneous since it does not allow the original fluid equations (4)–(6) to be satisfied. The correct interpretation of equations (14) is that the point $x = 1 + v$ is a singular point of the ordinary differential equations (11) and (12), and that for the flow to pass smoothly through such a singular point (if one exists), α must equal $2/x$ where $-v$ equals $1 - x$. For such solutions, nothing singular happens at the singular point, and the "singular point" is more appropriately referred to as a "critical point." Except for the aspects of self-gravity and time-dependence, the situation appears to be similar to Parker's (1963) discussion of the "nozzle conditions" in steady solar-wind flow, or to Bondi's (1952) discussion of the critical accretion rate in steady spherical-accretion flow. This analogy, however, turns out to be deceptive for the time-dependent problem. We show in the Appendix that solutions with critical points cannot generally represent the gravitational collapse of isothermal spheres.

At large radii, physical collapse flows will have monotonic velocity profiles in regions which are removed from shocks. Let us label solutions with positive derivatives, $d(-v)/dx$, as plus solutions, and those with negative derivatives, as minus solutions. Some examples are plotted in Figure 2. The plus solutions with critical points (*dashed curves*) are potentially useful as the time-reversed counterparts of self-gravitating winds (see Appendix). The curve labeled "LP" is the time-reversed counterpart of the solution obtained by Larson (1969) and Penston (1969*a*), and it passes through the critical-point locus at $x = 2.33$. Their unreversed solution lies in the second quadrant and has the properties listed in § I. With one important exception (see Appendix and § II*c*), the minus solutions with critical points (*dotted curves*) also cannot be used to describe collapse flows. Hence, we are motivated to investigate the properties of minus solutions without critical points.

b) Collapse Solutions without Critical Points

Shown in Figure 2 as light solid curves are minus solutions without critical points. These solutions are obtained by imposing the reasonable condition that the fluid velocities are negligible at the "initial instant," i.e., that $v \to 0$ as $x \to \infty$. It is a trivial matter to show from equations (11) and (12) that solutions which have this property have the asymptotic behaviors

$$\alpha \sim A/x^2\,, \quad v \sim -(A - 2)/x\,, \quad m \sim Ax \text{ as } x \to \infty\,, \tag{15}$$

where A is a constant whose value must be greater than 2 if we are to have inflow (v negative). Clearly, equation (15) requires that the initial density distribution have the self-similar form

$$\rho(r, 0) = \frac{a^2 A}{4\pi G}\, r^{-2}\,, \tag{16}$$

which corresponds to a singular isothermal sphere with a mass in excess of what it can have in hydrostatic equilibrium (cf. eq. [2]) if A is greater than 2. The physical interpretation of the result (15) is now obvious: collapse of the isothermal sphere (16) occurs if $A > 2$ because the local imbalance of gravity and pressure gradients everywhere can spontaneously generate inflow at every radii. (This behavior may be contrasted with the collapse of spheres which are initially in unstable hydrostatic equilibrium; see § II*c*.)

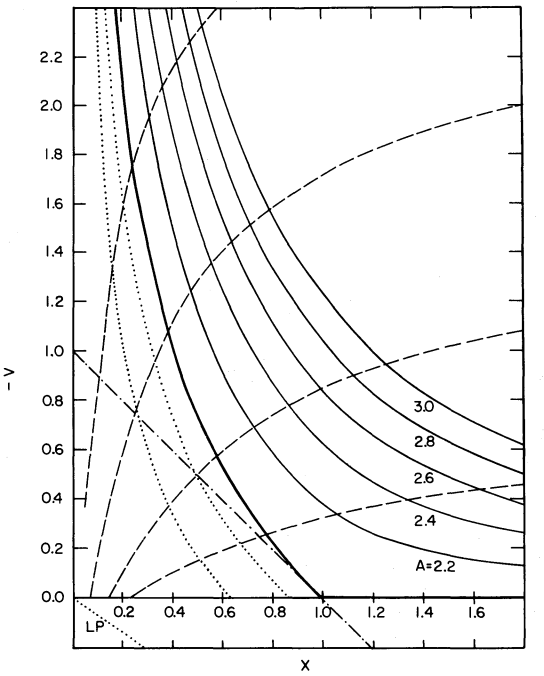

FIG. 2.—Similarity solutions for the reduced velocity in isothermal flow. The line inclined at −45° with respect to the x-axis gives the locus of the critical points: $-v = 1 - x$. Only the solid curves give acceptable solutions for the collapse problem; in particular, the heavy solid curve gives the collapse solution for a singular sphere which is initially hydrostatic ("expansion-wave collapse solution").

Although the minus solutions without critical points strictly apply only to the collapse of initial singular spheres whose density distributions are given by equation (16), the physical discussion of § I leads us to expect that all starting states which do not greatly exceed the condition (1) will approach asymptotically in time one of the similarity solutions corresponding to A somewhat greater than 2. Interpreted in this way, equation (15) implies that envelope density distributions develop an r^{-2} law in their outer parts so as to spread the discrepancy between gravity and pressure gradients as smoothly as possible. This dynamical explanation of the r^{-2} law is unrelated to various other explanations which have occasionally appeared in the literature.

The r^{-2} dependence of the density profile breaks down at small x. It is an easy matter to show from equations (11) and (12) that the minus solutions have the following behavior near the origin:

$$m \to m_0, \quad \alpha \to (m_0/2x^3)^{1/2}, \quad v \to -(2m_0/x)^{1/2} \quad \text{as } x \to 0. \quad (17)$$

Notice, therefore, that a smooth transition from subsonic flow to supersonic flow is made without the need to pass through a mathematical critical point. Time dependence (and self-gravity) distinguishes our solution from the classical accretion problem treated by Bondi (1952).

The physical interpretation of equation (17) is also obvious: at any time $t > 0$, an amount of reduced mass, m_0, has fallen into the core (protostar?), and the matter immediately above the core approaches a state of free-fall. The ratio of the gravitational acceleration to the pressure gradient acceleration is

$$\frac{GM}{r^2} : \frac{a^2}{\rho}\frac{\partial \rho}{\partial r} = \frac{m}{x^2} : \frac{d \ln \alpha}{dx} \to -\frac{3}{2}\frac{m_0}{x} \text{ as } x \to 0, \quad (18)$$

which increases without limit at finite t as $r \to 0$. This is the expected behavior. Of course, the real core has a finite but small size; hence, the solution (17) should be terminated at some very small value of x by introducing a shock. The location of the shock, the radiative precursor, and the optically thick, adiabatically compressed regions should be obtained by making a separate "inner calculation." We shall not discuss the point further except to note that the details of the "inner solution" cannot affect the external flow being discussed here which is incident on the core at supersonic speeds. In particular, the constant m_0 which represents the reduced mass of the core as well as the scaled mass accretion rate by the core (see eq. [8]) will be determined solely by the external flow.

The constant m_0 is, of course, related implicitly to the constant A in equation (15). This relationship can be discovered explicitly by numerical integration with starting conditions determined at large x by the asymptotic formulae (15). In practice, we have used the asymptotic series accurate to two orders in x^{-2} (α is an even function of x, and v is odd),

$$\alpha = \frac{A}{x^2} - \frac{A(A-2)}{2x^4} + \cdots,$$

$$v = -\frac{(A-2)}{x} - \frac{(1 - A/6)(A-2)}{x^3} + \cdots, \quad (19)$$

evaluated at $x = 10$ to provide starting conditions for a four-step Runge-Kutta integration scheme. The results for m_0 given A are tabulated in Table 1. To conserve space, we shall not give detailed tabulations of the functions $\alpha(x)$, $v(x)$, and $m(x)$ for different choices of the parameter A.

Of special interest, however, is the limiting case $A \to 2^+$. We have found that the solution obtained in this limit gives the same solution as the limit of the minus solutions with the limiting critical point $x_* \to 1^-$ discussed in the Appendix. The limiting solution is drawn in Figure 2 as the heavy solid curve, with equation (13) giving the behavior for $x \geq 1$. We call this special solution, the "expansion-wave collapse solution," and we explain its physical and mathematical properties in the next subsection.

c) *Expansion-Wave Collapse Solution*

The properties of the limiting collapse solution for $x \leq 1$ are tabulated in Table 2; the solution is given analytically by equation (13) for $x \geq 1$. We have obtained the results tabulated in Table 2 by quadratically extrapolating minus solutions with $A = 2.003$, 2.002, and 2.001 to the limit $A = 2^+$, with the explicit provision that the cloud is hydrostatic (at rest) for $x > 1$.

How are we to interpret the results of Table 2 physically? Imagine the following scenario. Construct a singular isothermal sphere in the precarious hydrostatic equilibrium governed by equation (2). At $t = 0$, introduce a perturbation which causes the central regions to collapse (e.g., molecule formation at the center of the cloud). The gravitational field and the density field in the outer layers remain unchanged; therefore, hydrostatic balance is maintained in the part of the envelope with $x > 1$. The layers immediately above the collapsing region ($x < 1$), however, soon find the bottom dropping out from beneath them, and they also begin to fall. The initiation of the falling process progresses outward in the form of an expansion wave (the flow solution for $x \leq 1$). The head of the expansion wave propagates at the speed of sound into a medium at rest; hence, its location is given by a sphere of radius $r_{\rm head} = at$, which corresponds to the value $x = 1$ for the similarity variable. The tail of the expansion wave is immediately outside of the origin, $x = 0$, where the material falls the fastest (free-fall). The reduced density α in the expansion wave between $x = 0$ and $x = 1$ drops below the equilibrium value, $2/x^2$. This density α, when multiplied by x^2 and integrated over $x = 0^+$ to $x = 1$, gives a reduced mass equal to 1.025. Thus, the reduced mass contained in the expansion wave, 1.025, plus the reduced mass

TABLE 1

RELATION BETWEEN A AND m_0

A....	2.00+	2.20	2.40	2.60	2.80	3.00	3.20	3.40	3.60	3.80	4.00
m_0...	0.975	1.45	1.88	2.31	2.74	3.18	3.63	4.10	4.58	5.08	5.58

which has already fallen into the core, $m_0 = 0.975$, gives a total reduced mass, m, contained inside $x = 1$ equal to 2—the original equilibrium value. The physical mass M contained in the expansion wave and in the core increases linearly with time (see eq. [8]); but the mass contained in the core at any instant t always comprises about 49% of the total mass contained within $r = at$.

The initial-value problem described above holds rigorously for all times only for the singular sphere (2) which extends to infinity. If we have a bounded singular sphere, the similarity solution begins to break down when the head of the expansion wave first hits the outer boundary (see § III). Moreover, the collapse of the marginally unstable Bonnor-Ebert sphere cannot be exactly self-similar because the initial envelope density distribution is not exactly that of the singular sphere (see Fig. 1). Nevertheless, an expansion-wave–initiated collapse of a form similar to the one discussed in this subsection must apply to all of the hydrostatic but unstable Bonnor-Ebert configurations discussed in § I. In this sense, the similarity solution given here serves as the prototype of all collapse calculations which start with hydrostatic states, just as the similarity solutions given in § II*b* serve as the prototype for all collapse calculations which start with masses that exceed the critical Bonnor-Ebert mass (1) only slightly. Collapse calculations which start with masses very much in excess of the Bonnor-Ebert critical mass will be better approximated by the analytic solutions for pressure-free collapse (with arbitrary density profiles) than by the similarity solutions given in this paper.

III. A NUMERICAL EXAMPLE

Our deliberations of § II (see especially Fig. 2) emphasize the basic expansion-wave nature of the collapse process in the envelopes of clouds which start out close to hydrostatic equilibrium. The expansion wave is created by the dropping of the central regions from beneath the envelope. Since the dense central regions collapse virtually in free-fall while the outer parts of the envelope can be influenced by the expansion wave only at the speed of sound, a massive core forms well before the collapse of the outer envelope.

To illustrate more graphically this basic process, we consider the specific numerical case, $a = 0.2$ km s^{-1}, corresponding roughly to the conditions appropriate to Bok globules or to the central regions of a nonmagnetic molecular cloud. For sake of definiteness, we follow the common practice of imposing a constant-pressure external boundary condition: we choose $P_{\rm ext}/k = 1.1 \times 10^5$ cm^{-3} K. We remark, however, that the choice of a constant-pressure boundary condition implicitly assumes that the sound speed in the external medium is much larger than the sound speed of our cloud.

Let us proceed by assuming the initial density distribution to be given by the singular isothermal sphere (2). To satisfy the outer boundary condition, we must truncate the singular solution (2) at $r = 1.6 \times 10^{17}$ cm $= 0.052$ pc. The mass contained within this radius, which is bounded by $P_{\rm ext}$, is $0.96\ M_\odot$. Given the low internal temperatures which have been assumed, the small mass of the object, and our previous remark concerning the assumed nature of the external medium, it would seem to be reasonable to identify our object as a Bok globule embedded in an H II region (Bok, Cordwell, and Cromwell 1971). Such objects may, however, be dubious candidates for star formation (Spitzer 1968); we return to this point later.

In any case, let us proceed at $t = 0$ to initiate gravitational collapse at the center of our object. Figures 3*a* and 3*b* give the subsequent collapse history of the density and velocity fields. The similarity solution of § II*d* governs the collapse until $t = 8 \times 10^{12}$ s $= 2.5 \times 10^5$ yr, at which time the head of the expansion wave first reaches the outer boundary. The subsequent evolution of the system—not drawn in Figures 3*a* and 3*b*—will see the internal pressure inside the boundary drop below the ambient value. Consequently, we can expect a compression wave to form at the boundary

TABLE 2

EXPANSION-WAVE COLLAPSE SOLUTION

x	α	$-v$	m	x	α	$-v$	m
0.00.....	∞	∞	0.975	0.55.....	3.66	0.625	1.30
0.05.....	71.5	5.44	0.981	0.60.....	3.35	0.528	1.36
0.10.....	27.8	3.47	0.993	0.65.....	3.08	0.442	1.42
0.15.....	16.4	2.58	1.01	0.70.....	2.86	0.363	1.49
0.20.....	11.5	2.05	1.03	0.75.....	2.67	0.291	1.56
0.25.....	8.76	1.68	1.05	0.80.....	2.50	0.225	1.64
0.30.....	7.09	1.40	1.08	0.85.....	2.35	0.163	1.72
0.35.....	5.95	1.18	1.12	0.90.....	2.22	0.106	1.81
0.40.....	5.14	1.01	1.16	0.95.....	2.10	0.051	1.90
0.45.....	4.52	0.861	1.20	1.00.....	2.00	0.000	2.00
0.50.....	4.04	0.735	1.25				

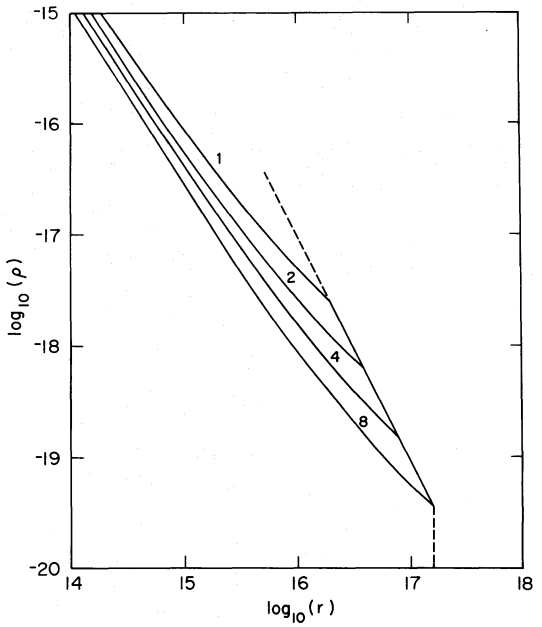

FIG. 3*a*

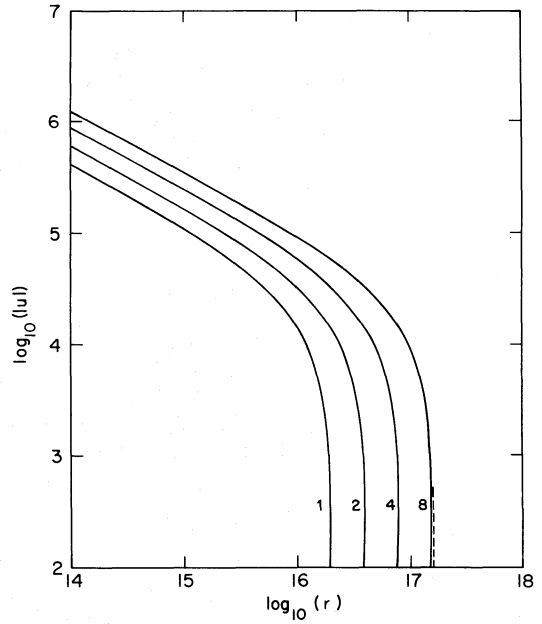

FIG. 3*b*

FIG. 3.—Expansion-wave collapse solution for a 0.96 $M_\odot$ singular sphere with $a = 0.2$ km s^{-1} and $P_{ext}/k = 1.1 \times 10^5$ cm^{-3} K. The initial radius of the outer boundary is indicated by the vertical dashed lines. (*a*) The density profiles at $t =$ 1, 2, 4, and 8 $\times$ 10^{12} s. (*b*) The velocity profiles at $t = 1$, 2, 4, and 8 $\times$ 10^{12} s. The dimensions of r, ρ, and u are cm, g cm^{-3}, and cm s^{-1}, respectively.

and to steepen into a shock wave as it propagates into the interior. This shock wave will help to push the rest of the infalling material in the envelope into the central core. The end state, thus, will consist of a 0.96 $M_\odot$ protostar embedded in the external medium (the H II region of another star?). The mass of the core at the instant of the formation of the compression wave is 0.47 $M_\odot$. It remains to be seen how important the effects of the compression wave are for the dynamics of the 0.49 $M_\odot$ which still remains in the envelope and which already has substantial inward motion and a pressure gradient that increases sharply toward the center.

The curves of Figures 3*a* and 3*b* corresponding to $t = 8 \times 10^{12}$ s may profitably be compared with Figure 10 of Larson (1972) which gives the envelope density and velocity fields at the instant when the core of his numerical hydrodynamic-code calculation has accumulated half of the mass of a collapsing 1 $M_\odot$ cloud. It can be seen that our curves are virtually identical to Larson's curves, except for the detailed behavior at the head of the expansion wave. This difference is attributable to the different initial and boundary conditions assumed by Larson. Clearly, the initial and boundary conditions are unimportant for the bulk of the flow which exhibits the self-similar properties described in the present paper. In particular, the inner envelope exhibits the power-law dependences, $\rho \propto r^{-3/2}$, $u \propto r^{-1/2}$, associated with free-fall collapse at steady mass accretion rates (see eq. [17]).

Little would be served by further discussion of this example. We wish, however, to make the following point. In the above collapse calculation, we obtain a stellar mass object only by resorting to a rather artificial setting. If we had not chosen such a low value of a and if we had not terminated our object by some artificial boundary pressure, but allow the equilibrium state to extend to considerably lower pressures, we would end up with very large masses for the central object. Under these circumstances, we must conclude that the initiation of the collapse of stellar mass objects cannot be considered a settled issue without a more careful investigation of the external boundary conditions and the assumption of spherical symmetric flow (see, e.g., Weber 1976). Fragmentation is often invoked as one hope; and it may be best to scale the present calculation to describe the collapse of a large interstellar cloud, bounded by the pressure of the intercloud medium, and within which the process of fragmentation into stellar mass objects might occur (Hunter 1967). As other promising examples, we quote Mouschovias's (1976) idea that the envelope of a magnetic molecular cloud might be prevented from falling onto the core by the tension associated with curved field lines, or Woodward's (1976) idea that the size of gravitationally unstable lumps in a large cloud might be determined by dynamic processes which occur behind galactic shocks. In any case, it is clear that the fundamental question of the masses of forming protostars has *not* been answered by *any* of the spherical gravitational collapse calculations performed to date—including the present one.

IV. DISCUSSION

In this paper, we have obtained similarity solutions which describe the gravitational collapse of isothermal

spheres that start as gas clouds not far removed from the condition of marginal stability. How can the discovery of these semianalytic solutions help to advance our theoretical concepts about the process of star formation? There seem to be at least two important applications.

First, there is the long-standing controversy over gravitational fragmentation (see the reviews by Layzer 1964 and by Hunter 1967). Hunter found that uniform pressure-free gas spheres undergoing collapse are unstable toward fragmentation. It would be useful to repeat the analysis for the self-similar collapse solutions. Although the latter solutions also reach free-fall conditions, the reduction of the pressure gradients in comparison with the gravitational forces is gained only at the expense of introducing very steep velocity gradients, and these extensional strains may provide a considerable stabilizing influence.

Second, there is also substantial controversy at present over whether the hydrostatic core (protostar) which is formed in the collapse process starts the pre–main-sequence stage of stellar evolution with dimensions close to a main-sequence star (Larson 1969, 1972; Appenzeller and Tscharnuter 1975), or two orders of magnitude larger (Narita, Nakano, and Hayashi 1970; Westbrook and Tarter 1975). The issue boils down to the amount of energy radiated away in the protostar formation process (Hayashi 1966, 1970).

To condense the argument, notice that after the dynamic collapse phase is over, we have a hydrostatic object (protostar). This object is a nearly fully-ionized gas, and it satisfies the virial theorem,

$$W + 2U = 0\,, \tag{20}$$

where W is the self-gravitational energy and U is the internal thermal energy. Independent of the details of the collapse process, we may relate the hydrostatic object to the original gas cloud from which it formed by an energy budget equation, which applies after the kinetic energy of collapse has been thermalized,

$$W + U + I + E_{\rm rad} = E_{\rm init}\,, \tag{21}$$

where I is the total energy required to break the molecules in the original cloud first into atoms and later into ions, where $E_{\rm rad}$ is the total energy radiated into space (and not into the protostar) during the dynamical collapse phase, and where $E_{\rm init}$ is the energy of the initial state. Clearly, $E_{\rm init}$ is many orders of magnitude smaller than the term W in equation (21); consequently, $E_{\rm init}$ can be set effectively to zero. If $E_{\rm rad}$ is similarly ignorable, the thermal energy U required to provide hydrostatic support for the object can be eliminated from expressions (20) and (21) to give

$$-W = 2I\,. \tag{22}$$

On the other hand, after the protostar contracts along a Hayashi track onto the main sequence, it satisfies the main-sequence virial theorem,

$$-W_{\rm m\text{-}s} = 2U_{\rm m\text{-}s}\,. \tag{23}$$

Now, the average thermal energy per hydrogen nucleus required to initiate nuclear burning in a main-sequence star is on the order of 10^3 eV, whereas the energy required to dissociate molecular hydrogen and ionize atomic hydrogen is on the order of 10^1 eV. Thus, the right-hand side of equation (23) is two orders of magnitude larger than the right-hand side of equation (22); and the radius R of the object—which is inversely proportional to W—would be roughly two orders of magnitude larger immediately after the dynamical collapse phase than at the corresponding main-sequence state.

To be able to obtain an initial hydrostatic object which has dimensions comparable to the main-sequence state requires $E_{\rm rad}$ in equation (21) to be larger than I by about two orders of magnitude. During the collapse phase, the energy radiated away by the infalling material is very small (a small fraction of an eV per particle) as long as the material remains cold; indeed, this fact explains why most of the gravitational energy released goes into producing free-fall motion. Hence, the only possibility of achieving large values of $E_{\rm rad}$ is via the radiating shock produced upon impact with the surface of the protostar. The structure of this radiative shock layer is calculated very crudely in the collapse calculations using hydrodynamic codes; hence, it should be possible to improve upon this crucial calculation if we could concentrate all of the computational effort on this thin but highly structured region of the flow. The similarity solutions derived in this paper provide just this possibility since they relieve us from the chore of calculating the external flow, which occupies the vast fraction of the volume of space but which presents a trivial contribution to the total energy balance.

I would like to thank Telemachos Mouschovias and Paul Woodward for some lively past discussions on the problems of star formation, and Lawrence Anderson, Steve Weber, and Charlie Westbrook for some helpful recent conversations. The encouragement of Bart Bok and Steve Strom in keeping active my interests in these problems is gratefully acknowledged. This research has been supported in part by NSF grant AST 75-02181. The numerical calculations for this paper were performed at the Berkeley Computing Center.

APPENDIX

THE PROPERTIES OF SOLUTIONS WITH CRITICAL POINTS

Let x_* denote the value of x, greater than zero, which corresponds to the singular point of the equations (11) and (12). A simple series expansion in the neighborhood of $x = x_*$ shows that the solution which passes smoothly

through x_*, with $d(-v)/dx$ positive if $x_* < 1$, has the form

$$-v = (1 - x_*) + \left(\frac{1}{x_*} - 1\right)(x - x_*) + \cdots, \qquad \alpha = \frac{2}{x_*} - \frac{2}{x_*}\left(\frac{3}{x_*} - 1\right)(x - x_*) + \cdots; \tag{A1}$$

whereas the solution which passes smoothly through x_*, with $d(-v)/dx$ negative if $x_* > 0$, has the form

$$-v = (1 - x_*) - \frac{1}{x_*}(x - x_*) + \cdots, \qquad \alpha = \frac{2}{x_*} - \frac{2}{x_*^2}(x - x_*) + \cdots. \tag{A2}$$

Thus, solutions with critical points are uniquely defined by the value of x_* and the designation of whether it is a solution of type (A1) or (A2). The continuation of these series solutions can be carried out by standard numerical techniques.

Each plus solution with a critical point of type (A1) (Fig. 2, *dashed curves*) asymptotically approaches a constant value for $-v$ at large x. Equation (12) then shows that the reduced density has the asymptotic behavior

$$\alpha \sim A/x^2 \text{ as } x \to \infty, \tag{A3}$$

where A is a constant which turns out to be less than 2 for the dashed curves. These gas spheres, therefore, have outer envelopes whose densities are *less* than the hydrostatic value; their time-reversed counterparts can represent self-gravitating winds. The r^{-2} dependence of the density field implied by equation (A3) clearly follows kinematically from the requirement of mass conservation for quasi-steady flow at uniform velocity.

The plus solution which satisfies the boundary condition $v \to 0$ as $x \to 0$ is especially interesting in the context of a wind solution for an isothermal sphere that expands into a vacuum. To investigate the properties of this solution near the origin, we find it convenient to introduce the reduced gravitational potential, ϕ, defined by

$$\frac{d\phi}{dx} = \frac{m}{x^2} = \alpha(x - v), \tag{A4}$$

where the second relation is implied by equation (10). In the approximation that $(x - v) \ll 1 \ll \alpha$, we can now integrate equation (12) to obtain the barometric formula

$$\alpha = e^{-\phi}. \tag{A5}$$

In equation (A5), we have absorbed the integration constant into the definition of ϕ, which is large and negative for small x. Using equation (A4), $v = x - e^{\phi} d\phi/dx$, to eliminate v, we easily obtain equation (11) in the approximate form,

$$\frac{1}{x^2}\frac{d}{dx}\left(x^2 \frac{d\phi}{dx}\right) = e^{-\phi}, \tag{A6}$$

which is the Lane-Emden equation for the isothermal sphere. Thus, the central regions of this similarity wind solution have, at each instant in time, the classic hydrostatic structure appropriate for isothermal spheres. We do not consider here the numerical problem of joining the approximate quasi-hydrostatic solution to the continuation of the series solution (A1) to small values of x.

Let us now consider the curve labeled "LP" in Figure 2. It corresponds to the time-reverse of the similarity solution found by Larson and Penston. Its behavior near the critical point is given by equation (A2) with $x_* = 2.33$, and its behavior at small x is given by

$$v \to \tfrac{2}{3}x, \quad \alpha \to 1.67, \quad m \to 0.56x^3 \qquad \text{as } x \to 0, \tag{A7}$$

while its behavior at large x is given by

$$v \to 3.3, \quad \alpha \to 8.9x^{-2}, \quad m \to 8.9x \qquad \text{as } x \to \infty. \tag{A8}$$

The boundary condition, $v \to 0$ as $x \to 0$, satisfied by equation (A7) is appropriate for wind solutions; however, the outer envelope is "overdense" (by a factor of 4.4 according to eq. [A8])—a characteristic we expect for collapse solutions. Moreover, the LP solution has the peculiar property that it is nowhere in hydrostatic equilibrium despite having a smooth profile everywhere. Thus, neither it nor its time-reverse has a meaningful interpretation in terms of either a collapse flow or a wind flow.

Let us finally consider the minus solutions with critical points of type (A2)—the dotted curves in Figure 2. These solutions intersect the x-axis, $-v = 0$, at some value of $x \leq 1$. Clearly these flows have vanishingly small spatial extent at small t unless we can extend the solution by some other means. The only sensible extension would join the singular solution (13) to the minus solutions at the x-intercept of the latter. Unfortunately, if we do this, we find

that the density α from the minus solution is generally smaller than the value of α obtained from the singular solution. Hence, the dotted minus solutions are useless for physically realistic accretion flows. The one exception to this rule is given by the joining of the minus solution corresponding to the limiting critical point, $x_* = 1^-$, with the singular solution. This exception is given by the solid heavy curve in Figure 2, and its properties are described in § II*c*.

REFERENCES

Appenzeller, I. 1972, *Mitt. Astr. Ges.*, **31**, 39.
Appenzeller, I., and Tscharnuter, W. 1975, *Astr. Ap.*, **40**, 397.
Bodenheimer, P., and Sweigart, A. 1968, *Ap. J.*, **152**, 515.
Bok, B. J., Cordwell, C. S., and Cromwell, R. H. 1971, in *Dark Nebulae, Globules, and Protostars*, ed. B. T. Lynds (Tucson: University of Arizona Press), p. 33.
Bondi, H. 1952, *M.N.R.A.S.*, **112**, 195.
Bonnor, W. B. 1956, *M.N.R.A.S.*, **116**, 351.
Chandrasekhar, S. 1957, *Stellar Structure* (New York: Dover Publications).
Ebert, R. 1955, *Zs. Ap.*, 217.
Gaustad, J. E. 1963, *Ap. J.*, **138**, 1050.
Hayashi, C. 1966, *Ann. Rev. Astr. Ap.*, **4**, 171.
———. 1970, in *Evolution Stellaire avant la Sequence Principale*, 16th Liège Symposium (Université de Liège), p. 127.
Hunter, C. 1967, in *Relativity Theory and Astrophysics 2. Galactic Structure*, ed. J. Ehlers (Providence: American Mathematical Society), p. 169.
Larson, R. B. 1969, *M.N.R.A.S.*, **145**, 271.
———. 1972, *M.N.R.A.S.*, **157**, 121.
———. 1973, *Ann. Rev. Astr. Ap.*, **11**, 219.
Layzer, D. 1964, *Ann. Rev. Astr. Ap.*, **2**, 341.
Lin, C. C., Mestel, L., and Shu, F. H. 1965, *Ap. J.*, **142**, 1431.
McNally, D. 1964, *Ap. J.*, **140**, 1088.
Mestel, L. 1974, in *Magnetohydrodynamics* (Geneva Observatory), pp. 116–150.
Mouschovias, T. Ch. 1976, *Ap. J.*, **207**, 141.
Narita, S., Nakano, T., and Hayashi, C. 1970, *Progr. Theor. Phys.*, **43**, 942.
Parker, E. N. 1963, *Interplanetary Dynamical Processes* (New York: Wiley).
Penston, M. V. 1969*a*, *M.N.R.A.S.*, **144**, 425.
———. 1969*b*, *M.N.R.A.S.*, **145**, 457.
Shu, F. H., Milione, V., Gebel, W., Yuan, C., Goldsmith, D. W., and Roberts, W. W. 1972, *Ap. J.*, **173**, 557.
Spitzer, L. 1968, in *Nebulae and Interstellar Matter*, ed. B. M. Middlehurst and L. H. Aller (Chicago: University of Chicago Press), p. 1.
Weber, S. V. 1976, *Ap. J.*, **208**, 113.
Westbrook, C. K., and Tarter, C. B., 1975, *Ap. J.*, **200**, 48.
Woltjer, L. 1972, *Ann. Rev. Astr. Ap.*, **10**, 129.
Woodward, P. R. 1976, *Ap. J.*, **207**, 484.

FRANK H. SHU: Astronomy Department, University of California, Berkeley, CA 94720